Journal of Structural Geology, Vol. 16, No. 1, pp. 61 to 70, 1994
Printed in Great Britain

0191-8141/94 $06.00+0.00

Kinematics of mylonitic rocks along the Median Tectonic Line, Akaishi Range, central Japan

HIROSHI YAMAMOTO*

Geological Institute, Faculty of Science, University of Tokyo, Hongo 7-3-1, Tokyo 113, Japan

(*Received* 2 *July* 1992; *accepted in revised form* 15 *February* 1993)

Abstract—The Ryoke Belt along the Median Tectonic Line (MTL) in the Akaishi Range is composed of quartz diorite, granodiorite and metasedimentary rocks in amphibolite facies. Microstructural evidence reveals that the quartz diorite and most of the metasedimentary rocks in the study area suffered a ductile shear deformation or a mylonitizaton. The shear surface is subhorizontal and the shear direction of the hanging wall trends N–S, based on the attitude of foliation and lineation of mylonitic rocks. Shear sense is deduced from microstructures such as mica 'fish' and asymmetric tails on porphyroclasts; they indicate relative southward displacement of the hanging wall. Comparison of deformation features in the described mylonites with those in fault rocks along the MTL, distribution of the mylonites, and kinematics of the mylonites and the MTL lead to the conclusion that the mylonites were mostly formed in a subhorizontal shear zone which was then exposed due to a dip-slip component of faulting on the MTL.

INTRODUCTION

THE Median Tectonic Line (MTL) is a major brittle fault zone dividing southwest Japan into the Inner Zone (continental side) and the Outer Zone (oceanic side). The MTL is traceable for about 1000 km, and is the longest fault zone in Japan. The MTL forms the boundary between two contrasting metamorphic belts, the high-*T*–*P* Ryoke Belt (Inner Zone) and the high-*P*–*T* Sanbagawa Belt (Outer Zone). The Ryoke Belt is characterized by high-*T*–*P* minerals such as andalusite–sillimanite, and is closely associated with intrusion of granitic rocks. The Sanbagawa Belt is characterized by high-*P*–*T* glaucophane-bearing schists. The two belts form a 'paired metamorphic belt' (Miyashiro 1961).

Mylonitic rocks occur in several areas in the Ryoke Belt along the MTL (Fig. 1; after Hayama & Yamada 1980). Protoliths of the mylonitic rocks are the Hiji Granite which is the oldest of the Ryoke granitic rocks, the younger Ryoke granitic rocks, and the Ryoke metamorphic rocks. All workers who studied mylonites along the MTL (e.g. Hayama *et al.* 1963, Hara *et al.* 1977, 1980, Hayama & Yamada 1980, Takagi 1984, 1986) have attributed the mylonitization directly to activity of the MTL, and its branch faults because: (1) the mylonitic rocks occur only within a distance of about 1 km from the MTL; (2) the degree of mylonitization becomes more intense towards the MTL; and (3) the most intensely mylonitized rocks occur adjacent to the MTL.

A few detailed analyses, on the other hand, have revealed that the geometry of mylonites can be different from that mentioned above. Mylonitic rocks are absent near Shinshiro, southeast of Nagoya where the MTL separates non-mylonitic granodiorite of the Ryoke belt from the Sanbagawa crystalline schist (Ikeda *et al.* 1974).

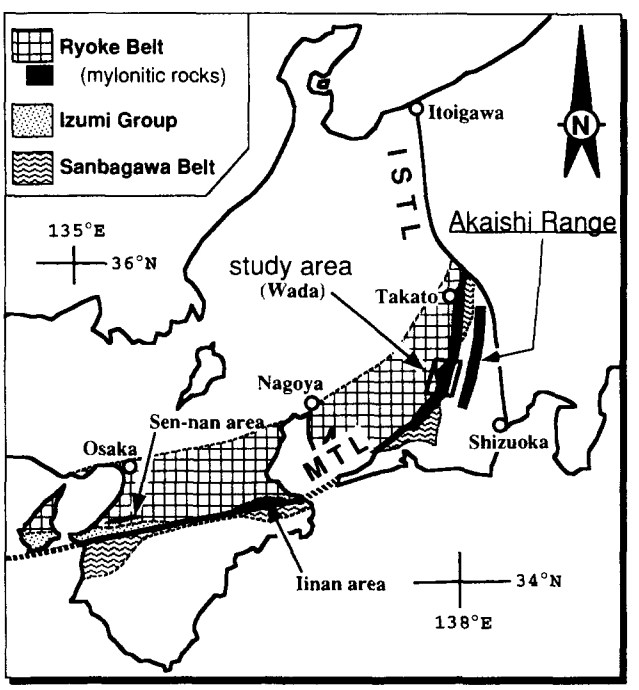

Fig. 1. Regional setting of the Median Tectonic Line and distribution of mylonitic rocks (shaded areas). MTL—Median Tectonic Line, ISTL—Itoigawa–Shizuoka Tectonic Line.

In the Iinan (Kayumi) area, east of Kii Peninsula, Echigo & Kimura (1973) showed that the mylonite in the Ryoke Belt is not confined to a narrow zone adjacent to the MTL but occurs at a distance of up to 5 km from the MTL, forming alternating zones of mylonites and non-mylonitic rocks parallel to the MTL. In the same area, Takagi (1985) described a shear zone (Inner Shear Zone) 3–5 km north of the MTL, in addition to the shear zone adjacent to the MTL. In the Sen-nan (Kishiwada) area west of the Kii Peninsula, the MTL is a boundary between sandstones of the Cretaceous Izumi Group and crystalline schists of the Sanbagawa Belt. No mylonites are present along the MTL here, but instead fault

*Current address: Institute of Earth Sciences, Faculty of Science, Kagoshima University, Kôrimoto 1-21-35, Kagoshima 890, Japan.

breccias and gouges are found. On the other hand, mylonitic rocks are present on a small area 10 km north from the MTL among the Ryoke granitic rocks (Yamada *et al.* 1979). Recently, Yamamoto & Masuda (1987, 1990) reported a mylonite zone adjacent to the subvertical MTL in Misakubo, central Japan, in which mylonites have a flat-lying mylonitic foliation. The occurrence of mylonitic rocks seems to be inconsistent with the strike-slip movement reported for the MTL. The purpose of this paper is to describe the macroscopic, mesoscopic and microscopic structures of the mylonitic rocks, and to re-examine the origin and structural relationship of these mylonitic rocks and the MTL.

GEOLOGICAL AND STRUCTURAL SETTING

The Akaishi Range is a rugged mountain chain which includes the second highest mountain (Peak Kitadake, 3192 m) in Japan. It extends over 50 km from north to south between the Itoigawa–Shizuoka Tectonic Line and the MTL. The studied area is located in the southwest of the Akaishi Range (Fig. 1).

The MTL strikes east-northeast in Shikoku and Kii Peninsula, north-northeast in the Akaishi Range, and north at its junction with the Itoigawa–Shizuoka Tectonic Line (Figs. 1 and 2). It dips steeply towards the north-northwest in Shikoku and Kii, and towards the east in the study area. The Sanbagawa crystalline schists are not exposed in the study area. Strata of the Outer Zone are composed of the Cretaceous Misakubo Formation, the Tertiary Wada Formation (Nakaseko *et al.* 1979) and the Mikabu Greenstone. The MTL actually crops out at two localities, Oshide and Aokuzure-toge in Fig. 2, where rocks of the Outer Zone and rocks of the Inner Zone are in direct contact. At Oshide, the MTL separates biotite–quartz schist of the Ryoke Belt from non-metamorphosed and non-mylonitized vitric-crystal tuff of the Outer Zone, and at Aokuzure-toge it separates quartz diorite of the Ryoke Belt from pyroxene gabbro of the Outer Zone. A zone of fault gouge 10–20 cm thick occurs immediately adjacent to the MTL, and the rocks of the Inner and Outer Zones are brecciated within a distance of several meters from the MTL.

The Inner Zone of the study area is occupied by metasediments of the Ryoke metamorphic sequence and quartz diorite and granodiorite of the Ryoke granitic assemblage (Fig. 2). The metasedimentary rocks are mica schists with variable mica content. The mica schists contain biotite, muscovite, quartz, plagioclase, garnet, sillimanite and andalusite. Sillimanite (fibrolite) and andalusite coexist in places (Fig. 3a). The pelitic mineral assemblage indicates metamorphism to the amphibolite facies. Rb–Sr and K–Ar isotopic ages from the Ryoke

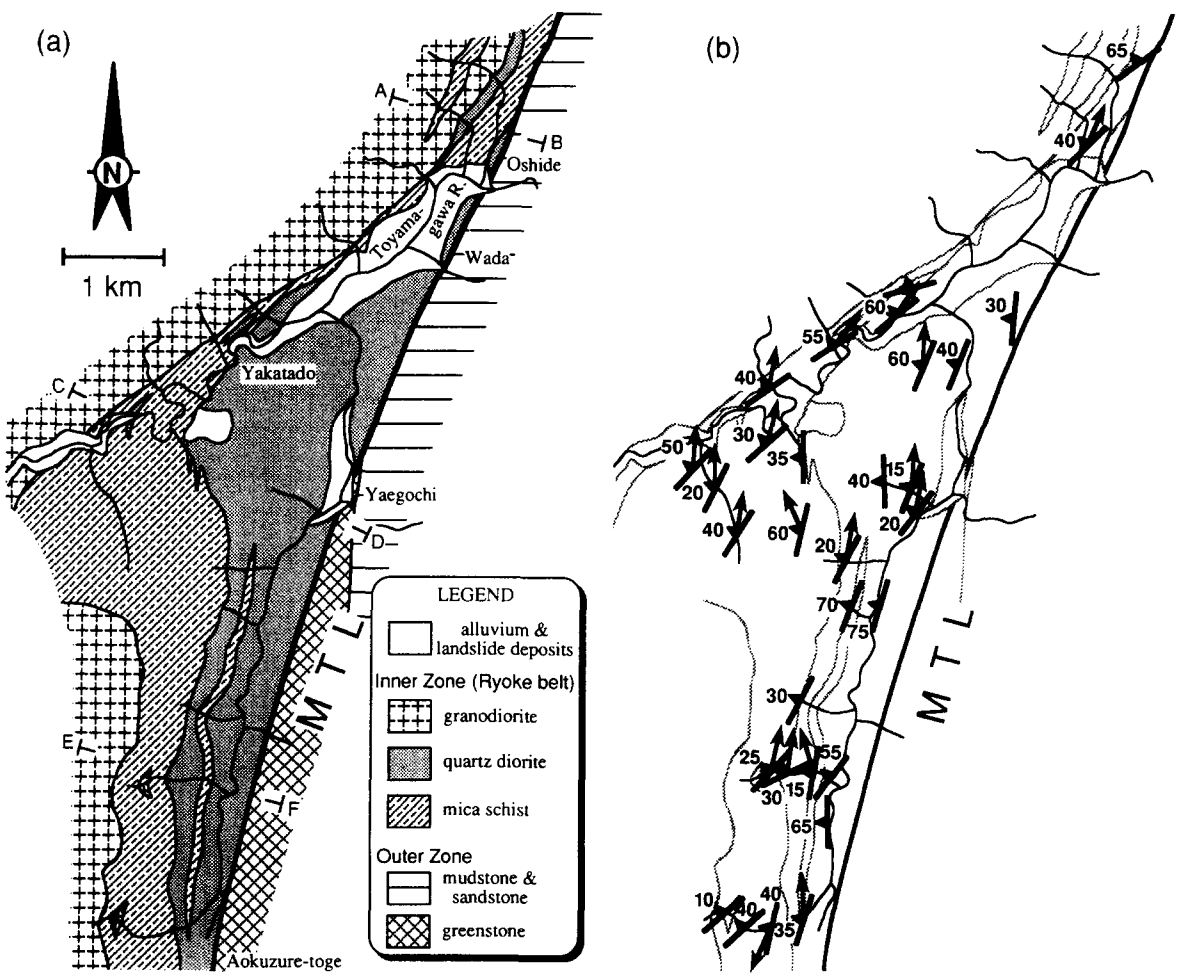

Fig. 2. (a) Geological map of the Ryoke belt along the MTL, Wada area. A–F mark locations of cross-sections shown in Fig. 4. (b) Structural map showing dip and strike of mylonitic foliation and azimuth of lineation (arrows) in the study area.

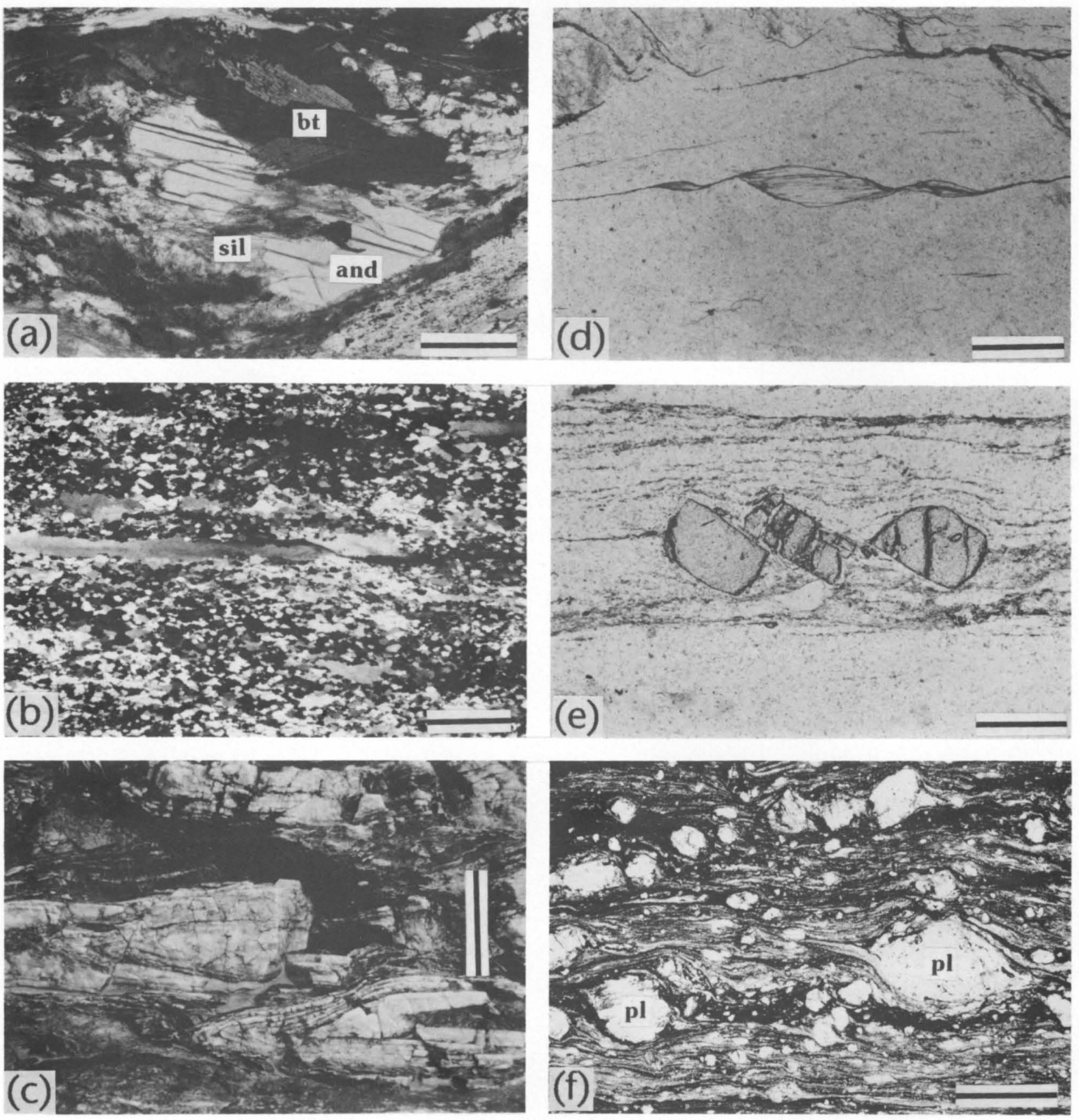

Fig. 3. Photographs showing mesoscopic and microscopic structures. Mineral abbreviations on the photographs: bt—biotite, sil—sillimanite, and—andalusite, pl—plagioclase. (a) Metamorphic index minerals in the mica schist. Section was cut normal to foliation and parallel to lineation (*XZ* section). Scale bar is 0.2 mm. Crossed polarized light. (b) Extensive dynamic recrystallization in metachert (*XZ* section). Scale bar is 0.5 mm. Crossed polarized light. (c) Isoclinal fold, metachert, Yakatado. Scale bar is 10 cm. (d) Asymmetric muscovite augen (mica 'fish') in the metachert indicating southward displacement (*XZ* section). Top is upward, and south is to the left. Scale bar is 0.5 mm. Plane polarized light. (e) Broken and aligned grains of garnet in the metachert indicating southward displacement (*XZ* section). Top is upward, and south is to the left. Scale bar is 0.2 mm. Plane polarized light. (f) Asymmetric tails on feldspar porphyroblasts in the quartz diorite indicating southward displacement (*XZ* section). Top is upward, and south is to the left. Scale bar is 3 mm. Crossed polarized light.

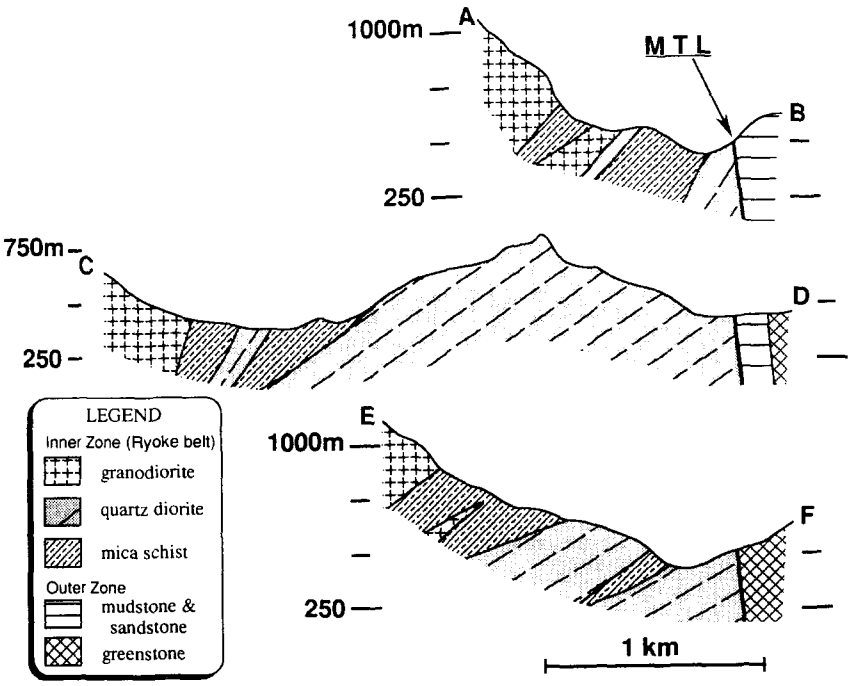

Fig. 4. Cross-sections across the MTL. See Fig. 2 for locations.

metamorphic rocks to the north of the study area range from 55 to 90 Ma (Harayama *et al.* 1985, Shibata & Takagi 1988). No isotopic dates have yet been obtained in the study area.

According to the Ryoke Research Group (1972), intrusion of the Ryoke granitic rocks occurred in nine phases during the Cretaceous period. The quartz diorite of the study area corresponds to the Hiji Granite of the first intrusive phase and the granodiorite corresponds to the Tenryukyo Granite of the second intrusive phase. The quartz diorite, which is situated at a relatively low structural level, has a relatively wide distribution in the central part of the study area where the rocks are excavated to a lower level than in the northern and southern parts (Fig. 2 and section C–D of Fig. 4). The quartz diorite is composed of quartz, plagioclase (An_{27-45}), hornblende and biotite with garnet, sphene, allanite and epidote as accessory minerals.

The granodiorite includes very coarse-grained (2–5 mm) porphyritic biotite granodiorite and coarse-grained gneissose biotite granodiorite. The former consists of large phenocrysts of feldspar and equidimensional matrix minerals. The latter has a weak gneissic fabric defined by aligned biotite flakes. The two types of the granodiorite have similar mineralogy; quartz, plagioclase, K-feldspar, biotite, muscovite, hornblende, and accessory minerals. Compared with the quartz diorite, the granodiorite is rich in K-feldspar and biotite and poor in hornblende. The quartz diorite first intruded into the mica schist, then the granodiorite intruded into both of quartz diorite and mica schist. Whole-rock Rb–Sr isotopic ages of the Older Granite, including the Hiji Granite and the Tenryukyo Granite dated by Kagami (1973), range between 265 and 110 Ma, and a Rb–Sr age reported by Yamana *et al.* (1983) is 90 Ma. Thus the intrusion of the Hiji Granite is inferred to pre-date or be coeval with the Ryoke metamorphism. Despite the

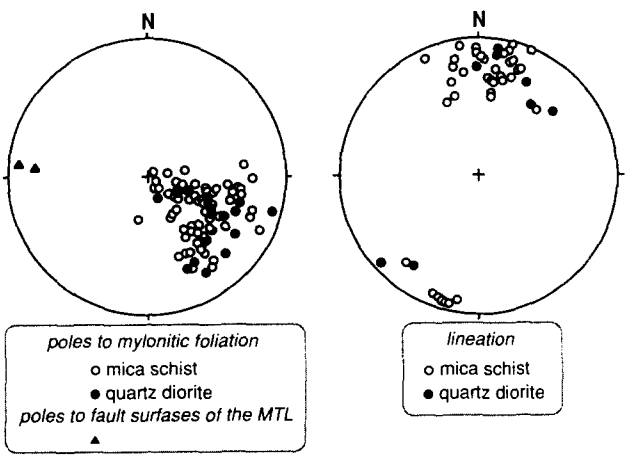

Fig. 5. Lower-hemisphere, equal-area projection of poles to mylonitic foliation and orientations of lineations.

broad range of whole-rock isotopic ages, most of biotite K–Ar and Ar–Ar ages from Ryoke granitic and metamorphic rocks are dated between 60 and 70 Ma indicating a similar cooling history for both (Harayama *et al.* 1985, Shibata & Takagi 1988, Dallmeyer & Takasu 1992). Since the closuring temperature of ^{40}Ar diffusion in biotite (*ca* 300°C, Harrison *et al.* 1985) is comparable with the lower temperature limit where quartz can be deformed significantly by the dislocation creep at geologically reasonable strain rates (Sibson 1977), the major stage of mylonitization would be dated at 60–70 Ma or older (Shibata & Takagi 1988, Dallmeyer & Takasu 1992).

A penetrative foliation parallel to compositional banding and a stretching lineation are present throughout the mica schist and the quartz diorite, but are rare and weak in the granodiorite. The foliation dips WNW at gentle to moderate angles, and the stretching lineation plunges N to NNE or SSW at 0–40° (Figs. 2b and 5).

The foliation is defined by aligned mica flakes, shape preferred orientation of ellipsoidal feldspar porphyroclasts, and flattened quartz aggregates. The lineation is defined by approximately parallel alignment of elongated grains of hornblende and plagioclase, and fine-grained mineral aggregates. The attitudes of the foliation and lineation in the mica schists are concordant with those in the quartz diorite. The foliation is discordant to the MTL as is clearly shown in cross-sections (Fig. 4). Dips of the foliation becomes gentler from north to south as shown in Fig. 4; they are steep in the section A–B, moderate in the section C–D, and relatively shallow in the section E–F.

The foliation and lineation are disrupted by later brittle deformation and alteration in a narrow zone adjacent to the MTL, where many veins with irregular orientation are developed in the quartz diorite. The veins are filled mostly by carbonate. Dark minerals such as biotite and/or hornblende and the groundmass are bleached to whitish green along the veins. Retrograde minerals such as sericite and chlorite occur in the altered quartz diorite and in the veins. In places, a complex of fine-grained carbonate veins with a thickness of several meters occur adjacent to the MTL.

MICROSCOPIC OBSERVATIONS

The foliation in sheared rocks is generally regarded to be parallel to the *XY* plane of finite strain, and the lineation defined by a dimensional preferred orientation of mineral grains is regarded to be parallel to the *X* direction of finite strain ellipsoid (Ramsay & Graham 1970, Hobbs *et al.* 1976). In this study, microscopic observations have been made on the *XZ* section. However, descriptions of the granodiorites are based on observation in sections of arbitrary direction because the granodiorites are weakly or non-foliated and non-lineated. Several kinds of 'asymmetric microstructures' which show monoclinic symmetry in the *XZ* section can be used for deducing the shear sense (e.g. Simpson & Schmid 1983, Lister & Snoke 1984). Some of these asymmetric microstructures are present in the mylonites studied and are described below.

Mica schist

The mica schist includes pelitic, psammitic and quartz schist in amphibolite facies. Deformation microstructures are clearly recognizable in banded quartz schist (metachert). The metachert was originally a bedded chert and is composed of an alternation of quartzose layers of several centimetres thick and micaceous layers of a few millimeters thick.

Quartz grains in the quartzose layers have both flattened and polygonal shapes. Strongly flattened quartz grains define the foliation. The flattened grains are a few millimeters in length and about 0.5 mm in width. They show undulatory extinction, deformation lamellae and consist of equidimensional subgrains (Fig. 3b). Flattened quartz grains have sutured grain boundaries due to grain boundary migration and new grain growth. Quartz grains with polygonal shape are smaller than 0.3 mm in diameter and do not show undulatory extinction. The boundary of individual grains is straight or slightly curved. A quartz polycrystalline aggregate with such a microstructure is commonly interpreted to result from crystal-plastic processes, especially dynamic-recrystallization (e.g. Bell & Etheridge 1973).

Micaceous layers in the metachert consist of sheaves of aggregates of subparallel lenticular biotite and muscovite up to 1 mm across. Individual mica flakes are 0.1–0.5 mm in length. In the hinges of isoclinal folds of metachert (Fig. 3c), mica flakes defining the older foliation are tightly crenulated. A new foliation defined by crenulated mica flakes is parallel to flattened quartz grains, with a spacing between 1 and 3 mm. The crenulation is irregular and disharmonic. In fold limbs, the mica sheaves are generally cross-cut by discrete microscopic shear zones (shear band and/or extensional crenulation cleavage; Platt & Vissers 1980). In the case of highly deformed sheaves, mica flakes are separated into asymmetric augen (mica 'fish', Fig. 3d) (Lister & Snoke 1984). The mica 'fish', resulting from boudinage and microfaulting of pre-existing large mica flakes during mylonitization, are widespread and are not restricted to a narrow zone adjacent to the MTL (Fig. 6) suggesting that the mylonitization affected the entire area occupied by the mica schist.

Individual mica 'fish' are linked by stair-stepped trails of very-fine, recrystallized mica (cf. Lister & Snoke 1984). In Fig. 3(d), stair-stepping of the mica 'fish' indicates a sinistral sense of shear (Lister & Snoke 1984).

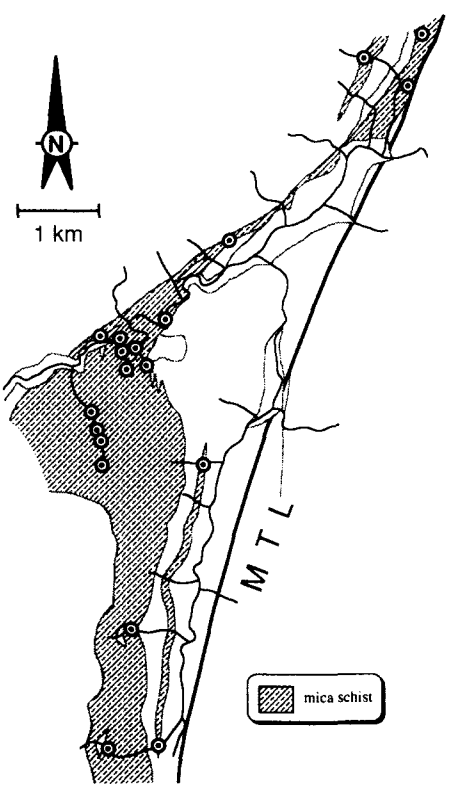

Fig. 6. Map showing distribution of mica 'fish' in the quartz schist (dotted circles).

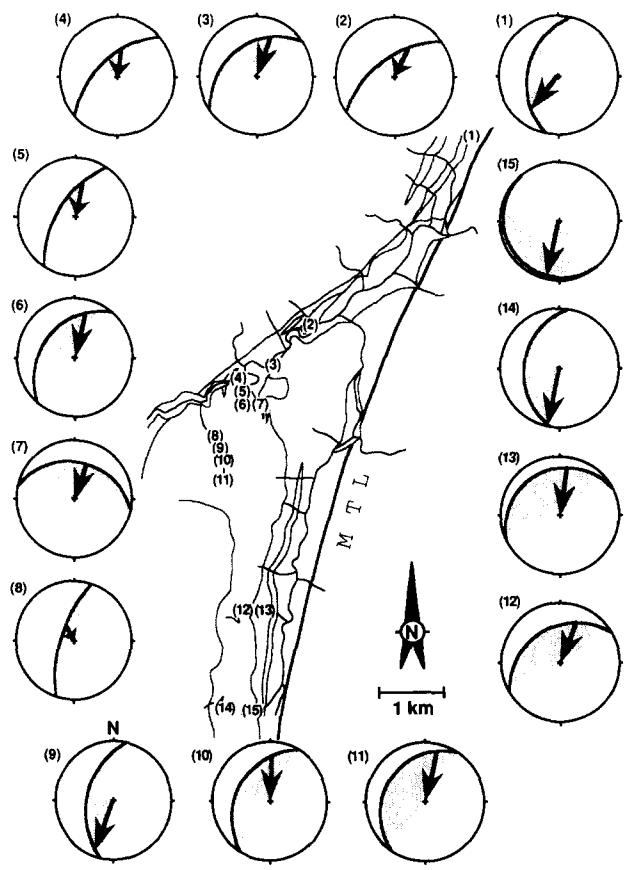

Fig. 7. Map showing displacement directions. Great circles are lower-hemisphere, equal-angle projections of the foliation. Arrows indicate relative displacement direction of the hanging wall.

All the mica 'fish' observed in oriented thin sections indicate that the hanging wall was displaced relatively southwards (Fig. 7).

Some feldspar and garnet porphyroclasts in pelitic and psammitic rocks have pull-apart fractures leading to the separation of porphyroclasts (Simpson & Schmid 1983). These fractures are filled with quartz, K-feldspar and minor amounts of biotite. Fracture surfaces are sharp and straight, and are mostly oriented at high angles to the foliation. When pull-apart fragments do not interact with other porphyroclasts, the fragments are aligned in an imbricated manner with respect to the mylonitic foliation (Fig. 3e). The imbrication of fragments also indicates southward shear sense as in the case of mica 'fish' (Fig. 7).

A pair of tails that are made up of recrystallized quartz, K-feldspar, biotite and muscovite are present on opposite sides of many porphyroclasts. Experimental and theoretical analyses of geometry of the tails have been reported in Passchier & Simpson (1986), Van Den Driessche & Brun (1987) and Masuda & Ando (1988). According to their results, the geometry of asymmetric tails observed in mica schist indicates southward shear sense.

Quartz diorite

Compositional banding of mafic and quartzo-feldspathic layers is well developed in the quartz diorite. The mafic layers are rich in hornblende, biotite and fine-grained opaque minerals. In quartzo-feldspathic layers, quartz grains form flattened lens-shaped aggregates of microgranular quartz. Each lens is 1–5 mm in length and 0.5–1 mm in width, and microgranular quartz is polygonal 0.01–0.1 mm in diameter. Individual quartz grains show no internal deformation features.

Plagioclase porphyroclasts have oblate or irregular shapes and are 0.2–5 mm across. Compositional zoning structure is preserved in some of the plagioclase porphyroclasts. Chemical composition of zoned plagioclase porphyroclasts were analyzed by the X-ray microprobe (JOUL JCMA 733 MKII wavelength-dispersive system at the Geological Institute, University of Tokyo, Japan). The cores of zoned plagioclase prophyroclasts have a higher anorthite content than the rims, of andesine composition (up to $An_{45\%}$). The anorthite content decreases toward the rim and is about 25% at the outer rim of the plagioclase porphyroclast. These porphyroclasts are presumably magmatic phenocrysts in origin, because within the porphyroclasts the outline of compositional zoning retains euhedral growth surfaces. Biotite and opaque minerals are commonly included in the porphyroclasts. Inclusions of biotite retain their undeformed tabular shape. Thus, it is inferred that the plagioclase porphyroclasts have considerably higher rigidity than quartz and are scarcely affected by plastic deformation.

Some plagioclase porphyroclasts have been cut into several fragments by pull-apart fractures. K-feldspar is the major mineral filling the fractures. K-feldspar also occurs on both sides of plagioclase porphyroclasts as pressure shadows. Where pull-apart fragments do not interact with other porphyroclasts, the fragments are aligned in an imbricated manner to the mylonitic foliation like the aligned fragments observed in the pelitic and psammitic rocks. These aligned fragments indicate southward displacement of the hanging wall. Asymmetric tails on porphyroclasts indicating southward shear sense are also observed (Fig. 3f).

Granodiorite

Little optical evidence for plastic deformation is observed in the porphyritic biotite granodiorite and the gneissose biotite granodiorite. The porphyritic granodiorite consists of phenocryst (up to 2 cm across) of K-feldspar, and smaller plagioclase, K-feldspar, biotite, hornblende and quartz grains (0.1–2 mm) with interlocked irregular boundaries. These minerals are randomly oriented and have no shape fabric. Twin lamellae and euhedral zoning outline of plagioclase are preserved unbroken. Undulatory extinction is weak and only observed in a few quartz grains.

The gneissose biotite granodiorite consists of subhedral to anhedral quartz and plagioclase, K-feldspar grains up to 2 mm across, and biotite and hornblende grains up to 1 mm across. The gneissosity is defined by a shape preferred orientation of biotite flakes and tabular sheaves of biotite aggregates. Quartz or quartz aggregates do not have a shape preferred orientation. The

aligned biotite flakes are surrounded by non-aligned anhedral quartz aggregates. Twin lamellae and euhedral zoning outlines of plagioclase are preserved unbroken. These observations suggest a magmatic origin of the gneissosity, not a mylonitic origin (e.g. Paterson *et al.* 1989).

GRAIN SIZE ANALYSIS

The main effect of mylonitization is a grain-size reduction of rock forming mineral grains. With regard to granitic rocks, quartz is most sensitive to grain size reduction (Bell & Etheridge 1973). The grain size of quartz has been used as an indicator to classify mylonitic rocks along the MTL. According to Hara *et al.* (1977, 1980) and Takagi (1986), the mean grain size of quartz in mylonitic rocks of the Ryoke Belt collected from several routes close to the MTL decreases toward the MTL. However, the lithology of the Ryoke Belt near the MTL is strongly variable and lithological boundaries are roughly parallel to the MTL. Because their study-sections traverse several lithological boundaries, the mean grain size measured by Hara *et al.* (1977, 1980) and Takagi (1986) does not necessarily reflect the intensity of mylonitization.

In this study, analyzed samples were collected along a route roughly perpendicular to the MTL (Fig. 8). The route traverses two different lithologic units, the granodiorite and the quartz diorite, in order to compare the difference in grain size between them. The mean grain size of quartz was measured in each thin section, in which the individual grains were selected exclusively from flattened lenses made up of polycrystalline quartz in order to avoid boundary effects caused by the other mineral grains.

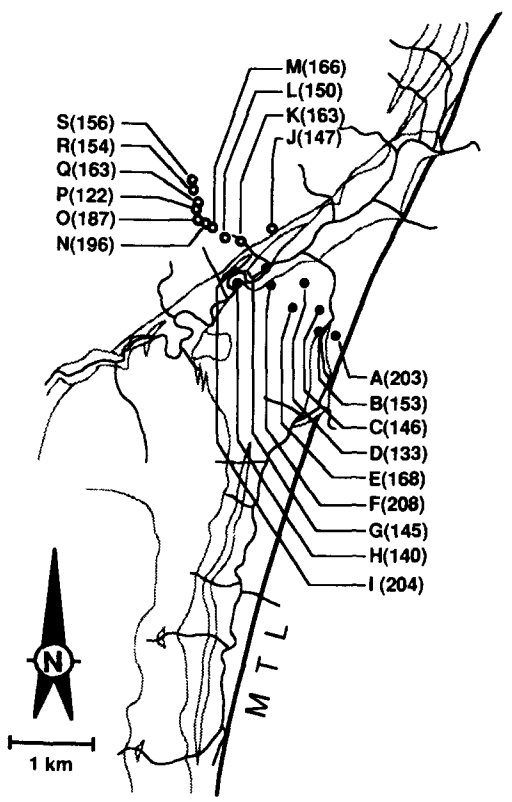

Fig. 8. Sample locality map. Open circles: granodiorites, Solid circles: quartz diorite. Numbers of measured quartz grains in each shin section are shown in brackets after locality letter.

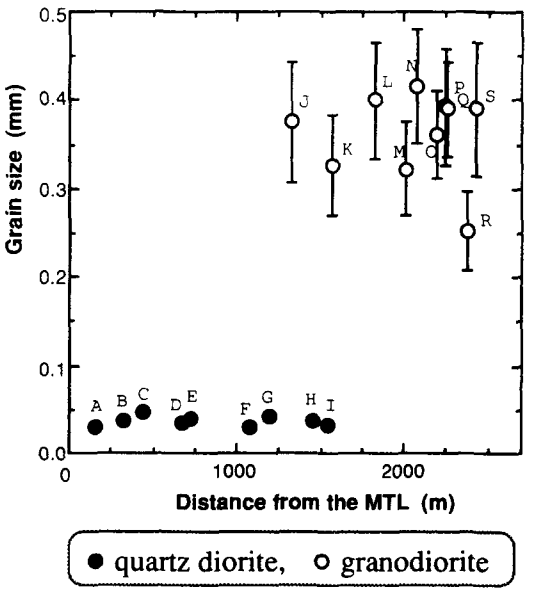

Fig. 9. Relationship between the mean grain size of quartz and distance from the MTL. Error bars represent 95% confidence interval. The dimensions of the plot symbols without error bars exceed the 95% confidence interval.

The mean grain size is defined by:

$$s = \frac{1}{n}\sum_{i=1}^{n} 2\sqrt{\frac{a_i}{\pi}}, \qquad (1)$$

where a is the area occupied by the individual grains, n is the number of measured grains in each thin section, and grain size is given as the arithmetical mean of diameter of circles on an equal area with measured grains. The NEXUS 6400 image analysis system (Kanagawa 1990) was used to collect a and n values from outline sketches of individual grains. Figure 9 gives the relationship between the mean grain size of quartz and distance from the MTL. The mean grain size measured in the quartz diorite ranges between 0.029 and 0.047 mm, and that measured in the granodiorite ranges between 0.252 and 0.416 mm. No systematic decrease of grain size toward the MTL is recognized from Fig. 9. The granodiorite and the quartz diorite that are situated at a nearly equal distance from the MTL do have significantly different grain sizes. The mean grain size of quartz changes abruptly across the lithological boundary and does not depend on the distance from the MTL. The quartz diorite is rather uniformly mylonitized, regardless of the distance from the MTL.

DISCUSSION AND CONCLUSION

The metasediments and the quartz diorite of the Wada area are separated from sediments and igneous

rocks of the Outer Zone by the MTL. The fault surface of the MTL is subvertical and trends NNE–SSW, although the attitude of mylonitic foliation dips moderately to gently toward the northwest or west. Asymmetric microstructures in the mylonitic rocks indicate southward displacement of the hanging wall. Although the abovementioned structural framework seems to be incompatible with the strike-slip kinematics reported for the MTL, it can be consistently explained by recent contributions on rheological properties of the crust.

Sibson (1977) described a model of deformation mechanisms in a fault zone in which the crust is divided into two layers; an upper elastico-frictional layer and a lower quasi-plastic layer. The two layers, more appropriately referred to as rheological regimes, are separated by a brittle–ductile transition zone (BDTZ). In a quartzo-feldspathic crust, the BDTZ probably corresponds roughly with the 300°C isotherm, marking the lower temperature boundary to greenschist-facies metamorphic conditions, where quartz begins to deform significantly by dislocation creep (Sibson 1977). The depth of the BDTZ is critically dependent on the local geothermal gradient and strain rate. According to Ord & Hobbs (1989), the BDTZ for the quartzo-feldspathic crust is situated at around 10 km depth if the geothermal gradient is 30°C km^{-1} and strain rate is 10^{-12} s^{-1}. Beneath the BDTZ, the Byerlee's (1968) relation for friction of rocks breaks down and the shear resistance of rocks decreases exponentially. If the local geothermal gradient is high, the BDTZ is situated at a shallow level in the crust, and the upper elastico-frictional layer is relatively thin (Ord & Hobbs 1989). Sibson (1983) has pointed out that an upper crustal 'flake' can detach from the lower crust bounded by the BDTZ in association with regional dip-slip faulting. In fact, thrust zones or normal fault zones which converge into flat-lying detachment zones have been reported from several orogenic belts (e.g. Coney 1980, Bally 1981, Rehrig 1986). In the case of strike-slip fault zones, Sibson (1983) suggested three alternative vertical profiles: (1) constant width; (2) downward widening; or (3) decoupling with depth. He favored downward widening based mainly on geological evidence. Some ancient strike-slip fault zones do show width increase with depth (e.g. Sorenson 1983, Hanmer 1988). With regards to the rheologically layered crust, it is not likely that a vertical strike-slip fault zone penetrates far downward into the quasi-plastic layer for a long period of time. This idea is strongly supported by recently published seismic images of some intracontinental strike-slip faults. The seismic images suggest that the strike-slip faults are decoupled in the middle crust by subhorizontal detachments (Cheadle *et al.* 1986, Lemiszki & Brown 1988).

In the study area, it is inferred from the presence of both andalusite and sillimanite, and absence of kyanite in the pelitic schist, that the geothermal gradient during metamorphism was higher than 30°C km^{-1}, and that the depth of BDTZ was less than 10 km. On the basis of the gently dipping shear surface, southward shear sense and the shallow BDTZ, a tentative vertical profile of the

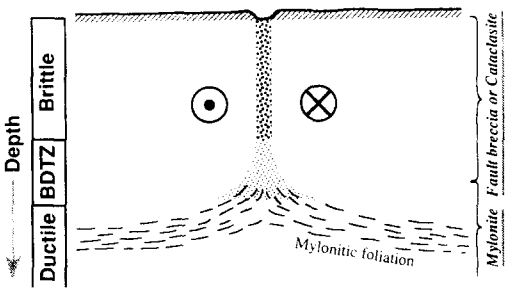

Fig. 10. Schematic illustration of a downward continuation of a strike-slip fault zone with rheological regimes: brittle, ductile and brittle–ductile transition zone (BDTZ). Modified from Sibson (1983).

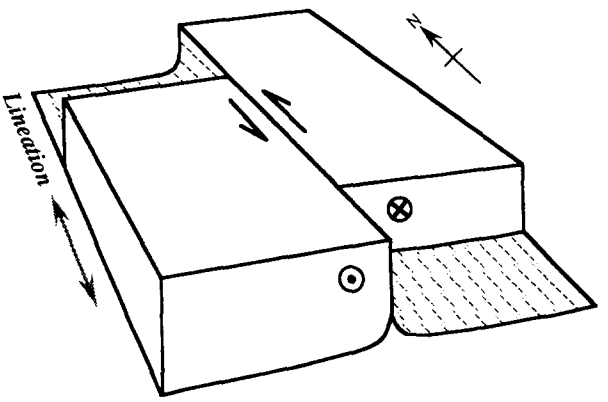

Fig. 11. Schematic block diagram showing inferred three-dimensional structure and relative motion of the overlying layer in the study area.

MTL and its movement picture when mylonitization took place may be as shown in Fig. 10, where a vertical strike-slip fault zone in the elastico-frictional layer diverges downward abruptly to a flat-lying shear zone. It is notable from the vertical profile that the segments of the elastico-frictional layer are separated by a strike-slip fault and are bounded by a subhorizontal shear zone at their base. According to this model, sinistral shear in the N–S-trending subvertical shear zone in the Takato area (Takagi 1984, 1986) is kinematically associated with the southward displacement in the subhorizontal shear zone in the Wada area (this study) as a southward displacement of the thin slab of the elastico-frictional layer that overrode on the western half of the fault zone (Fig. 11). This shear zone geometry closely resembles that of the San Andreas Fault System presented by Furlong *et al.* (1989), where a deeper shear zone connects with a surface fault system which has developed in the brittle regime.

The model presented here (Figs. 10 and 11) can explain why the occurrence of the mylonitic rocks is not always adjacent to the MTL (Echigo & Kimura 1973, Ikeda *et al.* 1974) and why the degree of mylonitization does not always become more intense toward the MTL (Yamamoto & Masuda 1987, 1990, Sakakibara *et al.* 1989). The presence or absence of mylonitic rocks is attributed to a difference in the level of uplift and erosion. The mylonitic rocks may be exposed in areas where the deep seated shear zone has been uplifted by a

dip-slip component of the later-stage strike-slip faulting and excavated by erosion.

Acknowledgements—I wish to express my sincere thanks to Dr S. Yoshida for his consistent guidance during this work. Drs T. Ito, A. Murata, K. Kanagawa and I. Shimizu provided very helpful suggestions. This paper benefitted from critical review by Dr C. K. Mawer and an anonymous reviewer.

REFERENCES

Bally, A. W. 1981. Thoughts on the tectonics of folded belts. In: *Thrust and Nappe Tectonics* (edited by McClay, K. & Price, N. J.). *Spec. Publs geol. Soc. Lond.* **9**, 13–32.

Bell, T. H. & Etheridge, M. A. 1973. Microstructure of mylonites and their descriptive terminology. *Lithos* **6**, 337–348.

Byerlee, J. D. 1968. Brittle-ductile transition in rocks. *J. geophys. Res.* **73**, 4741–4750.

Cheadle, B. L., Czuchra, T., Byrne, C. J., Ando, J. E., Olivier, J. E., Brown, L. D., Kaufman, S., Malin, P. E. & Phinney, R. A. 1986. The deep crustal structure of the Mojave desert, California, from CO-CORP seismic reflection data. *Tectonics* **5**, 293–320.

Coney, P. J. 1980. Cordilleran metamorphic core complexes: an overview. In: *Cordilleran Metamorphic Core Complexes* (edited by Crittenden, M. D., Coney, P. J. & Davis, G. H.). *Mem. geol. Soc. Am.* **153**, 7–31.

Dallmeyer, R. D. & Takasu, A. 1992. Middle Paleocene terrane juxtaposition along the Median Tectonic Line, southwest Japan: evidence from $^{40}Ar/^{39}Ar$ mineral ages. *Tectonophysics* **200**, 281–297.

Echigo, H. & Kimura, T. 1973. Minor geologic structures of the cataclastic rocks, including mylonites, along the Median Tectonic Line in the eastern Kii Peninsula, Southwest Japan. In: *The Median Tectonic Line* (edited by Sugiyama, R.). Tokai University Press, 115–137 (in Japanese with English abstract).

Furlong, K. P., Hugo, W. D. & Zandt, D. 1989. Geometry and evolution of the San Andreas Fault Zone in northern California. *J. geophys. Res.* **94**, 3100–3110.

Hanmer, S. 1988. Great Slave Lake Shear Zone, Canadian Shield: reconstructed vertical profile of a crustal-scale fault zone. *Tectonophysics* **149**, 245–264.

Hara, I., Yamada, T., Yokoyama, S., Arita, M. & Hiraga, Y. 1977. Study on the southern marginal shear belt of the Ryoke metamorphic terrain—Initial movement picture of the Median Tectonic Line. *Earth Sci. (Chikyu Kagaku)* **31**, 204–217 (in Japanese with English abstract).

Hara, I., Shyoji, K., Sakurai, Y., Yokoyama, S. & Hide, K. 1980. Origin of the Median Tectonic Line and its initial shape. *Mem. geol. Soc. Jap.* **18**, 27–49.

Harayama, S., Koido, Y., Ishizawa, K., Nakai, Y. & Kutsukake, T. 1985. Cretaceous to Paleogene magmatism in the Chubu district, Japan. *Earth Sci. (Chikyu Kagaku)* **39**, 345–357 (in Japanese with English abstract).

Harrison, T. M., Duncan, I. & McDougall, I. 1985. Diffusion of ^{40}Ar in biotite: temperature, pressure and compositional effects. *Geochim. cosmochim. Acta* **49**, 2461–2468.

Hayama, Y., Miyagawa, K., Nakajima, W. & Yamada, T. 1963. The Kashio Tectonic Zone, Urakawa to Wada Area, Central Japan. *Earth Sci. (Chikyu Kagaku)* **66**, 23–31 (in Japanese with English abstract).

Hayama, Y. & Yamada, T. 1980. Median Tectonic Line at the stage of its origin in relation to plutonism and mylonitization in the Ryoke Belt. *Mem. geol. Soc. Jap.* **18**, 5–26.

Hobbs, B. E., Means, W. D. & Williams, P. F. 1976. *An Outline of Structural Geology*. John Wiley, New York.

Ikeda, Y., Ui, H. & Sugaya, Y. 1974. A new exposure of the Median Tectonic Line at Shinshiro City, Aichi Prefecture. *J. geol. Soc. Jap.* **80**, 195–196 (in Japanese).

Kagami, H. 1973. A Rb–Sr geochronological study of the Ryoke Granites in Chubu district, central Japan. *J. geol. Soc. Jap.* **79**, 1–10.

Kanagawa, K. 1990. Automated two-dimensional strain analysis from deformed elliptical markers using an image analysis system. *J. Struct. Geol.* **12**, 139–143.

Lemiszki, P. J. & Brown, L. D. 1988. Variable crustal structure of strike-slip fault zones as observed on deep seismic reflection profiles. *Bull. geol. Soc. Am.* **100**, 665–676.

Lister, G. S. & Snoke, A. W. 1984. S–C mylonites. *J. Struct. Geol.* **6**, 617–638.

Masuda, T. & Ando, S. 1988. Viscous flow around a rigid spherical body: a hydrodynamical approach. *Tectonophysics* **148**, 337–346.

Miyashiro, A. 1961. Evolution of metamorphic belts. *J. Petrol.* **2**, 277–311.

Nakaseko, K., Matushima, N., Obata, I. & Matukawa, M. 1979. Geological age of the Misakubo and the Wada Formations in the Akaishi Mountains. *Mem. National Sci. Museum* **12**, 65–73 (in Japanese with English abstract).

Ord, A. & Hobbs, B. E. 1989. The strength of the continental crust, detachment zones and the development of plastic instabilities. *Tectonophysics* **158**, 269–289.

Passchier, C. W. & Simpson, C. 1986. Porphyroclast systems as kinematic indicators. *J. Struct. Geol.* **8**, 831–843.

Paterson, S. R., Vernon, R. H. & Tobisch, O. T. 1989. A review of criteria for the identification of magmatic and tectonic foliations in granitoids. *J. Struct. Geol.* **11**, 349–363.

Platt, J. P. & Vissers, R. L. M. 1980. Extensional structures in anisotoriopic rocks. *J. Struct. Geol.* **2**, 397–410.

Ramsay, J. G. & Graham, R. H. 1970. Strain variation in shear belts. *Can. J. Earth Sci.* **7**, 786–813.

Rehrig, W. A. 1986. Processes of regional Tertiary extension in the western Cordillere: Insights from the metamorphic complex. *Spec. Pap. geol. Soc. Am.* **208**, 97–122.

Ryoke Research Group 1972. The mutual relations of the granitic rocks of the Ryoke metamorphic belt in Central Japan. *Earth Sci (Chikyu Kagaku)* **26**, 205–216 (in Japanese with English abstract).

Sakakibara, N., Ohtomo, Y. & Hara, I. 1989. Structure of mylonitic rocks of the Ryoke belt in eastern part of the Kayumi district, Kii Peninsula. *Abs. 96th Ann. Meet. Geol. Soc. Japan* 278 (in Japanese).

Shibata, K. & Takagi, H. 1988 Isotopic ages of rocks and intrafault materials along the Median Tectonic Line—An example in the Bungui-toge area, Nagano Prefecture. *J. geol. Soc. Jap.* **94**, 35–50 (in Japanese with English abstract).

Sibson, R. H. 1977. Fault rocks and fault mechanisms. *J. geol. Soc. Lond.* **133**, 191–213.

Sibson, R. H. 1983. Continental fault structure and the shallow earthquake source. *J. geol. Soc. Lond.* **140**, 741–767.

Simpson, C. & Schmid, S. M. 1983. An evaluation of criteria to deduce the sense of movement in sheared rocks. *Bull. geol. Soc. Am.* **94**, 1281–1288.

Sorenson, K. 1983. Growth and dynamics of the Nordre Stromfjord shear zone. *J. geophys. Res.* **88**, 3419–3437.

Takagi, H. 1984. Mylonitic rocks along the Median Tectonic Line in Takato-Ichinise area, Nagano Prefecture. *J. geol. Soc. Jap.* **90**, 81–100 (in Japanese with English abstract).

Takagi, H. 1985. Mylonitic rocks of the Ryoke Belt in the Kayumi area, eastern part of the Kii Peninsula. *J. geol. Soc. Jap.* **91**, 637–651 (in Japanese with English abstract).

Takagi, H. 1986. Implications of mylonitic microstructures for the geotectonic evolution of the Median Tectonic Line, central Japan. *J. Struct. Geol.* **8**, 3–14.

Van Den Driessche, J. & Brun, J.-P. 1987. Rolling structure at large shear strain. *J. Struct. Geol.* **9**, 691–704.

Yamada, T., Hayama, Y., Kagami, H., Kutsukake, T. Maeno, S., Masaoka, K., Nakai, Y. & Yoshida, M. 1979. Geology of the Ryoke Belt in the Sennan district, Osaka Prefecture, Japan. *Mem. geol. Soc. Jap.* **17**, 211–222.

Yamamoto, H. & Masuda, T. 1987. Horizontal ductile shearing in mylonites of the Ryoke Belt in the Misakubo district, northwest Shizuoka Prefecture. *Abs. 94th Ann. Meet. Geol. Soc. Japan* 452 (in Japanese).

Yamamoto, H. & Masuda, T. 1990. Sub-horizontal ductile shearing in mylonites of the Ryoke Belt in the Misakubo district, northwest Shizuoka Prefecture. *Geosci. Repts. Shizuoka Univ.* **16**, 25–47 (in Japanese with English abstract).

Yamana, S., Honma, H. & Kagami, H. 1983. Nd and Sr isotopic study on the granitic rocks and the basic rocks of the Ryoke Belt. *Magma* **67**, 135–142 (in Japanese).